materials

MDPI

Article

Cobalt Oxide-Decorated Silicon Carbide Nano-Tree Array Electrode for Micro-Supercapacitor Application

Chuan-Pei Lee [1,2,*], Bayu-Tri Murti [1,3,4], Po-Kang Yang [4], Francesca Rossi [5], Carlo Carraro [2] and Roya Maboudian [2,*]

[1] Department of Applied Physics and Chemistry, University of Taipei, Taipei 10048, Taiwan; d96524014@ntu.edu.tw
[2] Berkeley Sensor & Actuator Center, Department of Chemical and Biomolecular Engineering, University of California, Berkeley, CA 94720, USA; carraro@berkeley.edu
[3] Graduate Institute of Biomedical Materials and Tissue Engineering, College of Biomedical Engineering, Taipei Medical University, Taipei 11031, Taiwan
[4] Department of Biomedical Sciences and Engineering, National Central University, Chung-li 32001, Taiwan; pkyang@ncu.edu.tw
[5] IMEM-CNR Institute, Parco Area delle Scienze 37/A, 43124 Parma, Italy; frossi@imem.cnr.it
* Correspondence: CPLee@utaipei.edu.tw (C.-P.L.); maboudia@berkeley.edu (R.M.)

Abstract: A cobalt oxide (Co_3O_4)-decorated silicon carbide (SiC) nano-tree array (denoted as Co_3O_4/SiC NTA) electrode is synthesized, and it is investigated for use in micro-supercapacitor applications. Firstly, the well-standing SiC nanowires (NWs) are prepared by nickel (Ni)-catalyzed chemical vapor deposition (CVD) method, and then the thin layer of Co_3O_4 and the hierarchical Co_3O_4 nano-flower-clusters are, respectively, fabricated on the side-walls and the top side of the SiC NWs via electrodeposition. The deposition of Co_3O_4 on the SiC NWs benefits the charge transfer at the electrode/aqueous electrolyte interface due to its extremely hydrophilic surface characteristic after Co_3O_4 decoration. Furthermore, the Co_3O_4/SiC NTA electrode provides a directional charge transport route along the length of SiC nanowires owing to their well-standing architecture. By using the Co_3O_4/SiC NTA electrode for micro-supercapacitor application, the areal capacitance obtained from cyclic voltammetry measurement reaches 845 mF cm^{-2} at a 10 mV s^{-1} scan rate. Finally, the capacitance durability is also evaluated by the cycling test of cyclic voltammetry at a high scan rate of 150 mV s^{-1} for 2000 cycles, exhibiting excellent stability.

Keywords: chemical vapor deposition; cobalt oxide; micro-supercapacitor; nanowire; silicon carbide

Citation: Lee, C.-P.; Murti, B.-T.; Yang, P.-K.; Rossi, F.; Carraro, C.; Maboudian, R. Cobalt Oxide-Decorated Silicon Carbide Nano-Tree Array Electrode for Micro-Supercapacitor Application. *Materials* **2021**, *14*, 4514. https://doi.org/10.3390/ma14164514

Academic Editors: Christian M. Julien and Boris Markovsky

Received: 28 June 2021
Accepted: 2 August 2021
Published: 11 August 2021

1. Introduction

Planar on-chip micro-supercapacitors are used as compact microscale, integrated, and reliable power sources for advanced microelectronics; meanwhile, they could also be integrated with microelectromechanical devices [1,2]. To date, various planar micro-supercapacitors have been studied in several papers [1–9]; the device-level integration of the electrode material is the major challenge of such devices. Among the electrode materials, carbonaceous materials are most commonly used for micro-supercapacitors, such as activated carbon [8,10], carbon nanotubes [3] and graphene [11], etc. However, these carbon-based materials are usually hydrophobic and result in poor surface wetting toward aqueous electrolytes; however, aqueous electrolytes are more environmentally friendly, stable, low-cost, and biocompatible than organic-based electrolytes. Accordingly, a promising electrode material, namely silicon carbide (SiC), has recently attracted considerable global interest in the field of aqueous electrolyte-based micro-supercapacitors, since it consists of abundant elements of earth and it has several excellent natures, such as superior durability under high current density and in various harsh conditions, high chemical stability and high mechanical strength [12,13]. Most importantly, it is more hydrophilic than the pristine

carbonaceous materials mentioned above [14–16]. On the other hand, it is well known that electrode materials having one-dimensional (1-D) nanostructure could provide extremely high specific surface areas, 1-D directional charge transport route, sufficient space for ion transfer, and structural stability during the charge/discharge processes [12,17–20]; those properties are desirable in capacitor applications. Accordingly, Chen et al. utilized a carbothermal reduction method to prepare SiC nanowire (NW) film on graphite paper to test its capacitive behavior [21]. The electrode with SiC nanowire film on graphite paper exhibits a specific capacitance of 37 mF cm^{-2} at 0.3 A cm^{-2}, and it also shows excellent capacity retention (i.e., 100%) after 2000 cycles. In our group, Alper et al. synthesized well-standing SiC NWs directly on a $SiC/SiO_2/Si(100)$ substrate as a highly robust electrode for micro-supercapacitor application [22]. Although the SiC NW electrode shows exceptional durability, i.e., 95% capacitance retention after 2×10^5 charge/discharge cycles at 5 V s^{-1} scan rate, its low areal capacitance of ~240 μF cm^{-2} measured at 100 mV s^{-1} still requires further improvement.

In this work, Co_3O_4 thin layer and hierarchical Co_3O_4 nano-flower-clusters are, respectively, fabricated on the side walls and the top side of the SiC NWs via the electrodeposition technique. The areal capacitance of the as-synthesized Co_3O_4/SiC nano-tree array (denoted as Co_3O_4/SiC NTA) electrode can reach 845 mF cm^{-2} at 10 mV s^{-1} scan rate; its durability is also evaluated by cyclic voltammetry for 2000 cycles at a high scan rate of 150 mV s^{-1}. Furthermore, the decoration of Co_3O_4 on SiC NWs not only provides high electrochemical activity, but also a low water contact angle that could remarkably improve the interface contact between electrode and aqueous electrolytes.

2. Materials and Methods

2.1. Synthesis of SiC NWs

The n-type 4H-SiC(0001) (Cree Research, Silicon Drive, NC, USA) wafer was used as the substrate for growing the SiC NWs on it. The 4H-SiC(0001) wafer were carefully cleaned before use, and the SiC NW arrays were prepared on the abovementioned substrate according to our previous reports, i.e., the Ni-catalyzed CVD method [12,22,23]. In brief, a ~2.5 nm Ni film was fabricated onto a cleaned 4H-SiC(0001) wafer substrate by using the electron beam evaporation; the as-prepared substrate was then transported into a hot-wall chemical vapor deposition (CVD) tube furnace to a base pressure of 30×10^{-3} Torr, wherein it was further heated to 950 °C at a rate of 50 °C min^{-1} at ~5 Torr under 10 sccm flow of H_2 (Praxair, 99.99%, Danbury, CT, USA). Once the furnace reached 950 °C, methyltrichlorosilane (MTS, Sigma-Aldrich, Saint Louis, MO, USA) was introduced into the reactor (0.5 sccm, 1 h); after that, the MTS source was turned off and the tube furnace was cooled down to ambient temperature under 10 sccm H_2 flow. The 4H-SiC(0001) wafer/SiC NWs electrode, denoted as the SiC NW array electrode hereafter, was thus prepared for this study.

2.2. Co_3O_4 Deposition

The Co_3O_4 deposition processes were carried out according to the previous report [12]. The Co_3O_4 was electro-deposited on the SiC NWs by using an electrochemical workstation (CH Instruments Inc., 660D, Bee Cave, TX, USA) at −0.9 V for 10 min in a three-electrode system. Before electro-deposition, the SiC NW array electrode was immersed in an isopropanol solution containing 1 M Cobalt(II) sulfate hydrate ($CoSO_4 \cdot xH_2O$; F.W. 155, Aldrich, USA) overnight and then rinsed with deionized water (DI-Water) and isopropanol (IPA, Sigma-Aldrich, USA) sequentially, and then dried by using N_2 gas. The as-pretreated SiC NW array electrode, a Ag/AgCl/saturated KCl(aq) and a Pt foil were used as the working, reference, and counter electrodes, respectively. The electro-deposition of Co_3O_4 was performed in 1 M $CoSO_4 \cdot xH_2O$ aqueous electrolyte. Finally, the Co_3O_4-deposited electrode was sintered under 350 °C for 1 h in air atmosphere. The Co_3O_4/SiC NTA electrode was thus prepared for this study.

2.3. Materials Characterization

The field emission scanning electron microscopy (FE-SEM, Nova Nano-SEM 230, FEI, Hillsboro, OR, USA) was utilized to observe the morphologies of the as-synthesized electrodes. A Horiba Jobin Yvon LabRam confocal Raman system (Horiba Jobin Yvon LabRam, excitation line provided by a HeNe laser at 632.8 nm, through a 100× objective with 0.8 numerical aperture) was used for Raman measurement. A JEOL-2100 transmission electron microscope (JEOL Ltd., Tokyo, Japan) was utilized to obtain the high-resolution transmission electron microscopy (HRTEM) images and the selected area electron diffraction (SAED) spectra under an acceleration voltage of 200 kV. The elemental distribution of Si, Co, and O in the Co_3O_4/SiC NTA was analyzed by energy dispersive X-ray spectroscopy (EDS) equipped on the TEM.

2.4. Electrochemical Characterization

Electrochemical measurements were carried out by using a potentiostat/galvanostat (PGSTAT 30, Autolab, Eco-Chemie, Utrecht, The Netherlands) with a three–electrode electrochemical cell containing an aqueous electrolyte of 5 M KOH. The as-pretreated Co_3O_4/SiC NTA electrode, a platinum sheet, and a saturated calomel electrode (SCE) reference electrode were used as the working electrode, counter electrode, and reference electrode, respectively. The areal capacitance was investigated by using cyclic voltammetry measurement at various scan rates [24].

3. Results and Discussion

The well-standing silicon carbide nanowires (designated as SiC NWs) were synthesized on SiC wafer substrates by a Ni-catalyzed CVD method, and then the Co_3O_4 was decorated on the SiC NWs to form Co_3O_4/SiC nano-tree arrays (denoted as Co_3O_4/SiC NTAs) via the electrodeposition technique. The as-prepared SiC NW film and Co_3O_4/SiC NTA film are first observed by field emission scanning electron microscopy (FE-SEM), as shown in Figure 1. Figure 1a,b show the top view SEM images of the SiC NW film and Co_3O_4/SiC NTA film, respectively. It can be seen that the top side of SiC NWs looks like a needle tip structure; after the electrodeposition of Co_3O_4, the hierarchical Co_3O_4 nano-flower-clusters appear on the top side of SiC NWs. The cross-section SEM images of above two samples are shown in Figure 1c,d. As shown in Figure 1c, the SiC NWs have directly grown on the substrate, and the thickness of the SiC NW film was around 15~17 μm. Furthermore, the SiC NW film is consisted of needle-like nanostructure with root diameter of ~230 nm at the bottom-side and ~10 nm at the top-side. In Figure 1d, we can obviously find that the top side of the SiC NWs was deposited with hierarchical Co_3O_4 nano-flower-clusters with irregular sizes and shapes. The high-magnification SEM images focusing on the partial region of Co_3O_4 nano-flower clusters from a cross-section view are shown in Figure 1e,f. In Figure 1e, the morphology shows a hierarchical structure with rough surface. In Figure 1f, a flower-like morphology is shown consisting of sheet structures. The as-prepared SiC NW film and Co_3O_4/SiC NTA film were further characterized by Raman spectroscopy (Figure 2). As shown in Figure 2a, the SiC NW film shows a hexagonal crystal structure composed of polytypes of SiC, and is predominantly 4H-like [23]. In Figure 2b, three sharp peaks at 658, 460, and 185 cm^{-1} were detected in the Raman spectrum of Co_3O_4/SiC NTA film; those peaks correspond to 1 A_{1g}, 1 E_g and 3 F_{2g} Raman active modes of Co_3O_4 [12,25,26]. As indicated in the previous report published by G. Varga et al. [27], both the Raman (Figure 2b) and X-ray diffraction (XRD, Figure S1 in the Supporting Information) measurements imply that a mixed spinel oxide structure could be produced via our synthesis route.

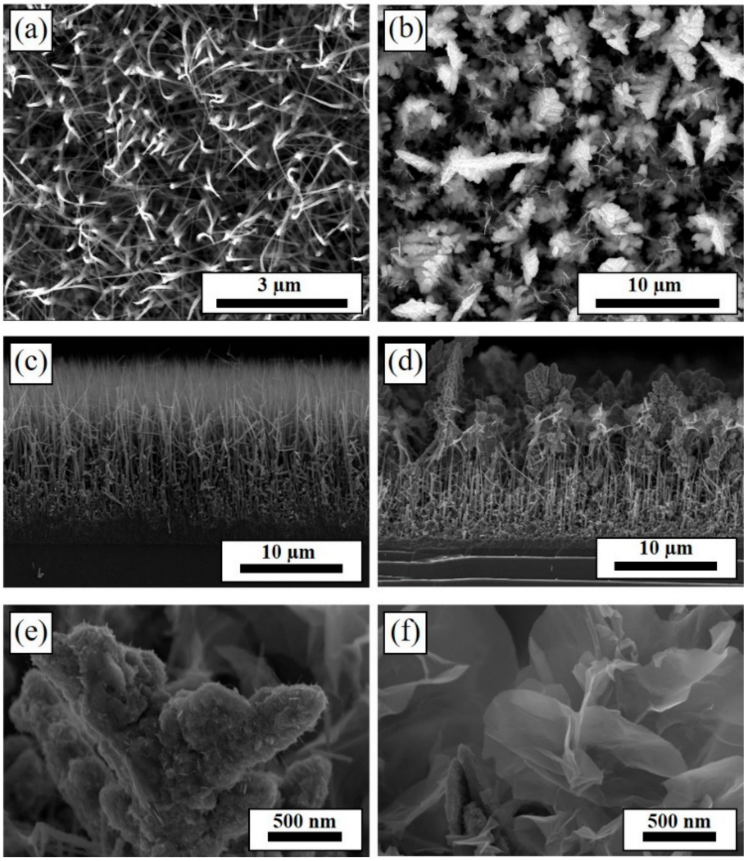

Figure 1. The top-view SEM images of the SiC NW film (**a**) before and (**b**) after Co_3O_4 decoration; their corresponding cross-section SEM images are shown in (**c**,**d**), respectively. (**e**,**f**) Are the high-magnification cross-section SEM images of the top side of (**d**).

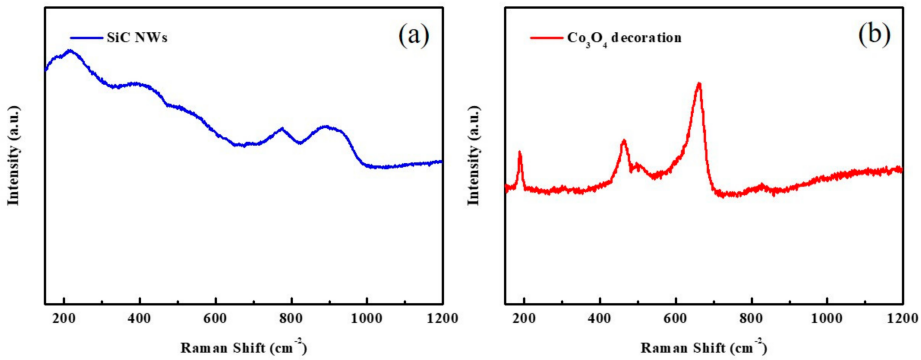

Figure 2. Raman spectra of (**a**) SiC NW film, and (**b**) Co_3O_4/SiC NTA film.

The HRTEM and EDS are further utilized to characterize the samples, as shown in Figures 3 and 4. Figure 3 shows the lattice fringe of a SiC NW, where a lattice spacing of about 0.25 nm can be assigned to the <111> lattice plane of SiC (i.e., along the c-axis of hexagonal polytypes or the <111> direction of the cubic polytype) [22,28]. As shown in the inset of Figure 3a, the typical streaking of reflections in this Fourier transform image confirm the presence of stacking faults along the NW axis; a high density of stacking faults associated with the presence of poly-types of SiC (i.e., mainly 3C-, 4H- and 6H-SiC). Figure 4a shows the TEM image of the Co_3O_4-decorated SiC NWs with Co_3O_4 sheets, and the enlarged image of the region in yellow dash frame is shown in Figure 4b. As shown in Figure 4b, the Co_3O_4 coating on the side-wall of SiC NW is conformal and continuous, and the thickness of the Co_3O_4 coating layer is around 7~18 nm. Moreover, the conformal and continuous characters of the Co_3O_4 coating is further verified by the

elemental distribution maps (Figure 4c–f) for a representation of the image shown in Figure 4b. Both Co and O characteristics of the Co_3O_4 are well distributed over the surface of SiC NW, revealing that the electrodeposition is effective for material loading onto high aspect-ratio nanostructures. We expect that the coating of Co_3O_4 layer on the surface of SiC NWs could distribute the charge flux evenly along the one-dimensional nanostructure of the SiC NWs, and the effective utilization of the high surface area of the SiC NWs would lead to less charge accumulation; both would facilitate the charge transfer kinetics in the electrochemical reaction.

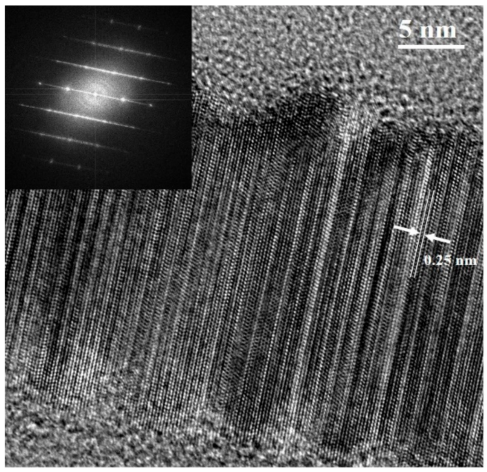

Figure 3. HRTEM image of a SiC NW with its corresponding selected area electron diffraction pattern (inset).

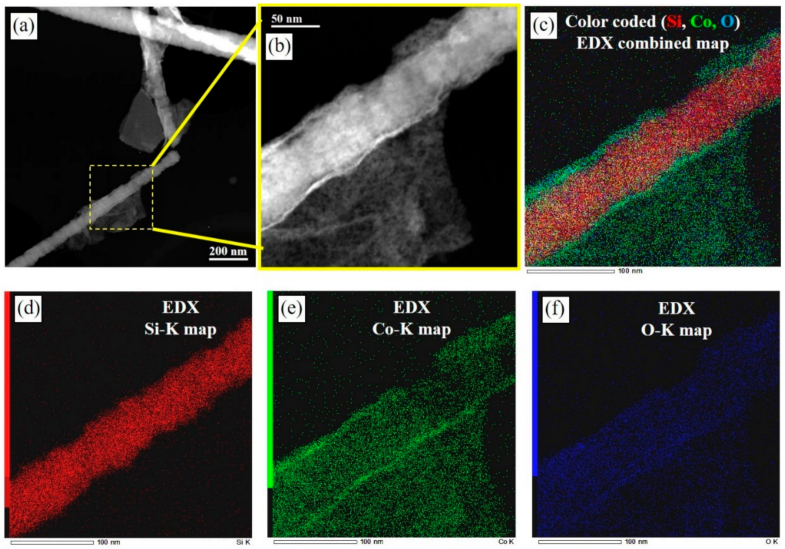

Figure 4. Selected TEM image of (**a**) the Co_3O_4-decorated SiC NWs with (**b**) Co_3O_4 nano-flower-clusters; the corresponding mapping image of (**b**) is shown in (**c**), and the individual elemental Si (red), Co (green), and O (blue) mapping images are shown in (**d**–**f**), respectively.

On the other hand, a zero-contact angle toward water droplets was observed on the SiC NW film was Co_3O_4 decoration, whereas the pristine SiC NW film shows a contact angle of ~60° (see Figure 5). The above results reveal that the water droplet can completely wet the surface of Co_3O_4/SiC NTA electrode and the surface is extremely hydrophilic, which would benefit the charge transfer at the interface of the aqueous electrolyte and the Co_3O_4/SiC NTA electrode. This advantage can be supported by the report [17], which demonstrated that the electrode exhibited lower contact angle toward water droplet usually

possesses lower charge transfer resistance at the interface between the electrode and the aqueous electrolyte.

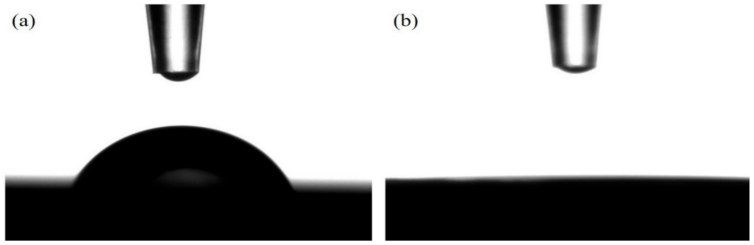

Figure 5. Surface contact angles of water droplets on the SiC NW film (**a**) before and (**b**) after Co_3O_4 decoration.

Figure 6a shows the variation of areal capacitance for different scan rates by using a Co_3O_4/SiC NTA electrode. All the areal capacitance values are extracted from the cyclic voltammetry curves, as shown in the inset of Figure 6a. As the scan rate increased, the current density increased; all cyclic voltammetry curves remain of similar shape even at high scan rates, suggesting that the inner area underneath the Co_3O_4/SiC NTA was able to contribute to the capacitance because of the hierarchical structure (i.e., the Co_3O_4 nano-flower-clusters and continuous/conformal Co_3O_4 coating on SiC NW arrays) developed inside the Co_3O_4/SiC NTA electrode. The areal capacitance values were calculated to be 845, 291, 218, and 182 mF cm^{-2} at scan rates of 10, 50, 100, and 150 mV s^{-1}, respectively. To evaluate the durability of the Co_3O_4/SiC NTA electrode, the cycling performance was tested under a high scan rate of 150 mV s^{-1}, and the obtained capacitance values in each cycle were plotted as a function of the cycle number (Figure 6b). Herein, we observed a negligible change on the capacitance of the Co_3O_4/SiC NTA electrode after 2000 cycles.

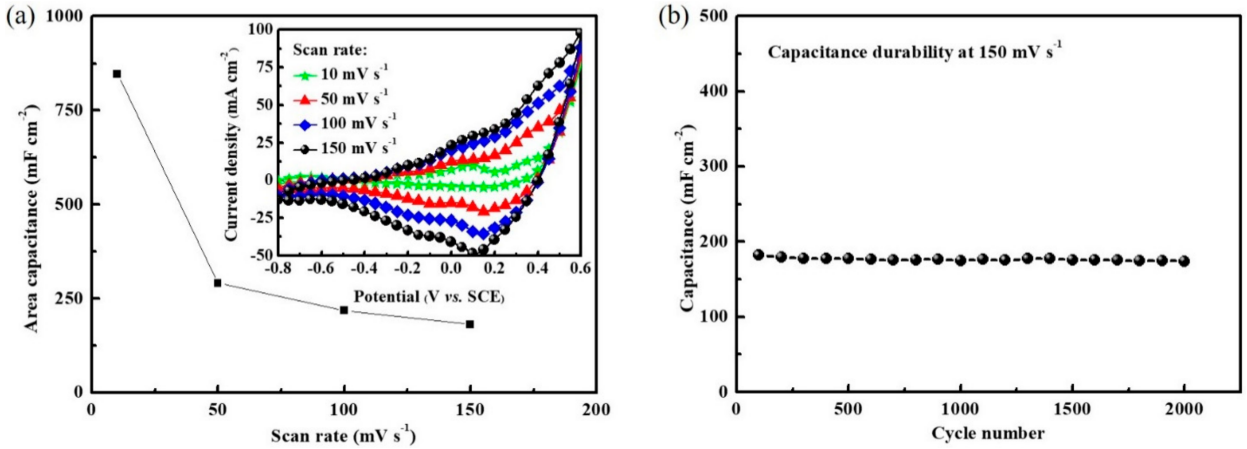

Figure 6. (**a**) Variation of areal capacitance for scan rate by using the Co_3O_4/SiC NTA electrode, which was obtained from the cyclic voltammetry curves, as shown in the inset. (**b**) The capacitance durability of Co_3O_4/SiC NTA electrode measured at 150 mV s^{-1}.

4. Conclusions

In summary, we synthesize an efficient Co_3O_4/SiC NTA electrode for application in micro-supercapacitors. By using the electrodeposition technique, a Co_3O_4 thin layer and hierarchical Co_3O_4 nano-flower clusters can be successfully decorated on the side walls and the top side of the SiC NWs, respectively. The areal capacitance of the as-prepared Co_3O_4/SiC NTA electrode can reach 845 mF cm^{-2} at 10 mV s^{-1}; moreover, its durability is also evaluated by the cycling test of cyclic voltammetry for 2000 cycles at a high scan rate of 150 mV s^{-1}. As compared to the previous report using the SiC NW-based electrode [21], the good performance of the Co_3O_4/SiC NTA electrode arises from the synergetic effects

between Co_3O_4 and SiC NW arrays. The SiC NW arrays provide a directional charge transport route along the nanowire length in the Co_3O_4/SiC NTA electrode, as well as high surface area for Co_3O_4 catalyst loading. Furthermore, the electro-deposited Co_3O_4 provides high electrochemical activity, and exhibits zero contact angle toward aqueous solutions that facilitates the interfacial contact between electrode and aqueous electrolyte. The concurrent advantage of earth-abundant constituent materials, good performance, and durability could make the Co_3O_4/SiC NTA electrode a viable candidate for micro-supercapacitor mass production.

Supplementary Materials: The following are available online at https://www.mdpi.com/article/10.3390/ma14164514/s1, Figure S1: The XRD (X-ray diffraction) patterns of the Co_3O_4 powder collected form the Co_3O_4/SiC NTA electrodes via ultrasonic. (a) Before and (b) after the cycling test of cyclic voltammetry.

Author Contributions: Experiment, C.-P.L. and B.-T.M.; Conceptualization and organization, C.-P.L., F.R., C.C. and R.M.; writing—original draft, C.-P.L., B.-T.M., P.-K.Y. and R.M.; material analysis, P.-K.Y. and F.R. All authors have read and agreed to the published version of the manuscript.

Funding: This research received funding from Ministry of Science and Technology (MOST) of Taiwan, under grant numbers 107-2113-M-845-001-MY3, 110-2113-M-845-002-MY2 and 109-2636-E-038-004; and US National Science Foundation (grant # 1903188).

Data Availability Statement: Data is available within the article.

Acknowledgments: This work was supported by the Ministry of Science and Technology (MOST) of Taiwan, under grant numbers 107-2113-M-845-001-MY3, 110-2113-M-845-002-MY2 and 109-2636-E-038-004. We would also like to thank the US National Science Foundation (grant # 1903188) and the industrial members of the Berkeley Sensor & Actuator Center (BSAC) for additional support of this project.

Conflicts of Interest: The authors declare no conflict of interest.

References

1. Beidaghi, M.; Wang, C. Micro-supercapacitors based on three dimensional interdigital polypyrrole/C-MEMS electrodes. *Electrochim. Acta* **2011**, *56*, 9508–9514. [CrossRef]
2. Patil, S.; Lee, D.-W. Status review on the MEMS-based flexible supercapacitors. *J. Micromech. Microeng.* **2019**, *29*, 093001. [CrossRef]
3. Jiang, Y.Q.; Zhou, Q.; Lin, L. Planar MEMS Supercapacitor using Carbon Nanotube Forests. In Proceedings of the 2009 IEEE 22nd International Conference on Micro Electro Mechanical Systems, Sorrento, Italy, 25–29 January 2009; pp. 587–590.
4. Li, P.; Shi, W.; Liu, W.; Chen, Y.; Xu, X.; Ye, S.; Yin, R.; Zhang, L.; Xu, L.; Cao, X. Fabrication of high-performance MXene-based all-solid-state flexible microsupercapacitor based on a facile scratch method. *Nanotechnology* **2018**, *29*, 445401. [CrossRef]
5. Jiang, Q.; Wu, C.; Wang, Z.; Wang, A.C.; He, J.-H.; Wang, Z.L.; Alshareef, H.N. MXene electrochemical microsupercapacitor integrated with triboelectric nanogenerator as a wearable self-charging power unit. *Nano Energy* **2018**, *45*, 266–272. [CrossRef]
6. Liu, F.; Gutes, A.; Laboriante, I.; Carraro, C.; Maboudian, R. Graphitization of n-type polycrystalline silicon carbide for on-chip supercapacitor application. *Appl. Phys. Lett.* **2011**, *99*, 112104. [CrossRef]
7. Alper, J.P.; Vincent, M.; Carraro, C.; Maboudian, R. Silicon carbide coated silicon nanowires as robust electrode material for aqueous micro-supercapacitor. *Appl. Phys. Lett.* **2012**, *100*, 163901. [CrossRef]
8. Pech, D.; Brunet, M.; Taberna, P.-L.; Simon, P.; Fabre, N.; Mesnilgrente, F.; Conédéra, V.; Durou, H. Elaboration of a microstructured inkjet-printed carbon electrochemical capacitor. *J. Power Sources* **2010**, *195*, 1266–1269. [CrossRef]
9. Chmiola, J.; Largeot, C.; Taberna, P.-L.; Simon, P.; Gogotsi, Y. Monolithic Carbide-Derived Carbon Films for Micro-Supercapacitors. *Science* **2010**, *328*, 480–483. [CrossRef]
10. Beidaghi, M.; Chen, W.; Wang, C. Electrochemically activated carbon micro-electrode arrays for electrochemical micro-capacitors. *J. Power Sources* **2011**, *196*, 2403–2409. [CrossRef]
11. Liu, C.; Yu, Z.; Neff, D.; Zhamu, A.; Jang, B.Z. Graphene-Based Supercapacitor with an Ultrahigh Energy Density. *Nano Lett.* **2010**, *10*, 4863–4868. [CrossRef]
12. Lee, C.-P.; Luna, L.E.; DelaCruz, S.; Ortaboy, S.; Rossi, F.; Salviati, G.; Carraro, C.; Maboudian, R. Hierarchical cobalt oxide-functionalized silicon carbide nanowire array for efficient and robust oxygen evolution electro-catalysis. *Mater. Today Energy* **2018**, *7*, 37–43. [CrossRef]
13. Yang, N.; Zhuang, H.; Hoffmann, R.; Smirnov, W.; Hees, J.; Jiang, X.; Nebel, C.E. Electrochemistry of Nanocrystalline 3C Silicon Carbide Films. *Chem. Eur. J.* **2012**, *18*, 6514–6519. [CrossRef]

14. Shang, X.; Zhu, Y.; Li, Z. Surface modification of silicon carbide with silane coupling agent and hexadecyl iodiele. *Appl. Surf. Sci.* **2017**, *394*, 169–177. [CrossRef]
15. Taherian, F.; Marcon, V.; van der Vegt, N.F.A.; Leroy, F. What Is the Contact Angle of Water on Graphene? *Langmuir* **2013**, *29*, 1457–1465. [CrossRef] [PubMed]
16. Kwak, B.; Park, S.; Lee, H.-S.; Kim, J.; Yoo, B. Improved Chloride Ion Sensing Performance of Flexible Ag-NPs/AgCl Electrode Sensor Using Cu-BTC as an Effective Adsorption Layer. *Front. Chem.* **2019**, *7*. [CrossRef] [PubMed]
17. Lee, C.-P.; Chen, W.-F.; Billo, T.; Lin, Y.-G.; Fu, F.-Y.; Samireddi, S.; Lee, C.-H.; Hwang, J.-S.; Chen, K.-H.; Chen, L.-C. Beaded stream-like CoSe2 nanoneedle array for efficient hydrogen evolution electrocatalysis. *J. Mater. Chem. A* **2016**, *4*, 4553–4561. [CrossRef]
18. Wang, K.; Xi, D.; Zhou, C.; Shi, Z.; Xia, H.; Liu, G.; Qiao, G. CoSe2 necklace-like nanowires supported by carbon fiber paper: A 3D integrated electrode for the hydrogen evolution reaction. *J. Mater. Chem. A* **2015**, *3*, 9415–9420. [CrossRef]
19. Faber, M.S.; Dziedzic, R.; Lukowski, M.A.; Kaiser, N.S.; Ding, Q.; Jin, S. High-Performance Electrocatalysis Using Metallic Cobalt Pyrite (CoS2) Micro- and Nanostructures. *J. Am. Chem. Soc.* **2014**, *136*, 10053–10061. [CrossRef]
20. Alper, J.P.; Gutes, A.; Carraro, C.; Maboudian, R. Semiconductor nanowires directly grown on graphene - towards wafer scale transferable nanowire arrays with improved electrical contact. *Nanoscale* **2013**, *5*, 4114–4118. [CrossRef]
21. Chen, J.; Zhang, J.; Wang, M.; Gao, L.; Li, Y. SiC nanowire film grown on the surface of graphite paper and its electrochemical performance. *J. Alloys Compd.* **2014**, *605*, 168–172. [CrossRef]
22. Alper, J.P.; Kim, M.S.; Vincent, M.; Hsia, B.; Radmilovic, V.; Carraro, C.; Maboudian, R. Silicon carbide nanowires as highly robust electrodes for micro-supercapacitors. *J. Power Sources* **2013**, *230*, 298–302. [CrossRef]
23. Luna, L.E.; Ophus, C.; Johansson, J.; Maboudian, R.; Carraro, C. Demonstration of Hexagonal Phase Silicon Carbide Nanowire Arrays with Vertical Alignment. *Cryst. Growth Des.* **2016**, *16*, 2887–2892. [CrossRef]
24. Kwak, J.H.; Lee, Y.-W.; Bang, J.H. Supercapacitor electrode with an ultrahigh Co3O4 loading for a high areal capacitance. *Mater. Lett.* **2013**, *110*, 237–240. [CrossRef]
25. Zhang, L.; Zhao, X.; Ma, W.; Wu, M.; Qian, N.; Lu, W. Novel three-dimensional Co3O4 dendritic superstructures: Hydrothermal synthesis, formation mechanism and magnetic properties. *CrystEngComm* **2013**, *15*, 1389–1396. [CrossRef]
26. Ding, Y.; Xu, L.; Chen, C.; Shen, X.; Suib, S.L. Syntheses of Nanostructures of Cobalt Hydrotalcite Like Compounds and Co3O4 via a Microwave-Assisted Reflux Method. *J. Phys. Chem. C* **2008**, *112*, 8177–8183. [CrossRef]
27. Varga, G.; Sápi, A.; Varga, T.; Baán, K.; Szenti, I.; Halasi, G.; Mucsi, R.; Óvári, L.; Kiss, J.; Fogarassy, Z.; et al. Ambient pressure CO2 hydrogenation over a cobalt/manganese-oxide nanostructured interface: A combined in situ and ex situ study. *J. Catal.* **2020**, *386*, 70–80. [CrossRef]
28. Liao, X.; Chen, J.; Wang, M.; Liu, Z.; Ding, L.; Li, Y. Enhanced photocatalytic and photoelectrochemical activities of SnO2/SiC nanowire heterostructure photocatalysts. *J. Alloys Compd.* **2016**, *658*, 642–648. [CrossRef]